Noninvasive in-vivo glucose detection in human finger interstitial fluid using wavelength-modulated differential photothermal radiometry

*Xinxin Guo, Di Zhang, Khashayar Shojaei-Asanjan, Koneswaran Sivagurunathan, Alexander Melnikov, Peng Song, and Andreas Mandelis**

*Corresponding author: e-mail mandelis@mie.utoronto.ca, phone +1 416-978-5106

Center for Advanced Diffusion-Wave and Photoacoustic Technologies (CADIPT), Department of Mechanical and Industrial Engineering, University of Toronto, 5 King's College Road, Toronto, ON M5S 3G8, Canada

Key words: noninvasive glucose detection, biosensor, diabetes management, photothermal effect, Quantum Cascade Lasers

We present a noninvasive and noncontacting biosensor using Wavelength Modulated Differential Photothermal Radiometry (WM-DPTR) to monitor blood glucose concentration (BGC) through interstitial fluid (ISF) probing in human middle fingers. WM-DPTR works in the interference-free mid-infrared range with differential wavelengths at the peak and baseline of the fundamental glucose molecule absorption band, giving rise to high glucose sensitivity and specificity. In vivo WM-DPTR measurements and simultaneous finger pricking BGC reference measurements were performed on diabetic and nondiabetic volunteers during oral glucose tolerance testing (OGTT). The measurement results demonstrated high resolution and large dynamic range (~ 80 degree) change in phase signal in the normal-to-hyperglycemia BGC range (5 mmol/L – higher than 33.2 mmol/L), which were supported by negative control measurements. The immunity to temperature variation of WM-DPTR yields precise and accurate noninvasive glucose measurements in the interstitial fluid.

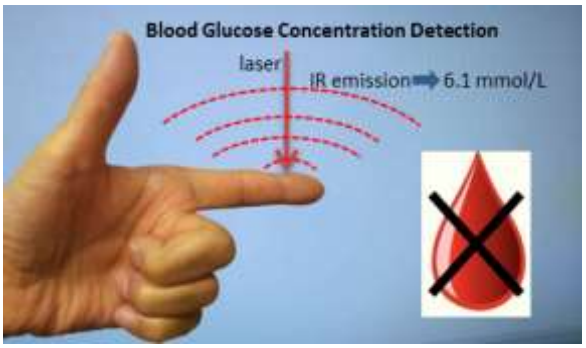

Modulated Differential Photothermal Radiometry (WM-DPTR).

1. Introduction

Diabetes is a chronic, progressive disease and an important public health problem. The number of people with diabetes worldwide has been steadily rising, from 108 million in 1980 to 422 million in 2014 and it is expected to exceed 654 million within the next 25 years [1,2]. Diabetes management through tight blood glucose control can improve the life quality of diabetic patients [3]. The finger pricking test is currently the most common technique used for blood glucose monitoring. However, it is painful and inconvenient, which hinders frequent testing and thus affects diabetes management. A noninvasive, needle-free alternative to the finger pricking test would be desirable for diabetes patients. For this reason, great efforts have been expended to develop noninvasive devices for decades [4]. The main technologies used for noninvasive glucose monitoring can be divided into two groups: (1) optical methods, such as near-infrared (NIR) and mid-infrared (MIR) absorption spectroscopy, Raman and photoacoustic spectroscopy [5-10]; (2) transdermal methods, such as impedance spectroscopy, reverse iontophoresis and ultrasound [11-13]: Optical techniques utilize light interacting with glucose in a concentration-dependent

This article has been accepted for publication and undergone full peer review but has not been through the copyediting, typesetting, pagination and proofreading process, which may lead to differences between this version and the Version of Record. Please cite this article as doi: 10.1002/jbio.201800441

manner, but the major limitation is the effect of the properties of the investigated tissue such as skin colour and photon scattering. Transdermal techniques involve the measurement of body fluid glucose through the skin using either electricity or ultrasound. However, they are easily affected by environmental variables e.g. temperature and sweat. Thermal techniques have also been developed [14,15]. Although there has been much research toward developing a noninvasive glucose monitoring device, there exist no truly noninvasive technologies to replace finger pricking to-date.

Wavelength-Modulated Differential Photothermal Radiometry (WM-DPTR) developed by our group is a noninvasive and non-contacting technique for measuring minute absorptions of low-concentration solutes in strongly absorbing fluids like water and blood [16]. It works in the MIR range, coincident with the fundamental glucose absorption band. Our previous in vitro measurements have demonstrated WM-DPTR to be an ultrasensitive technique for glucose detection [17-20]. In this paper we present accurate in vivo glucose concentration measurement results from human finger interstitial fluid (ISF) probing using WM-DPTR during oral glucose tolerance testing (OGTT).

2. Material and methods

2.1 Theory

WM-DPTR is a real-time differential method utilizing out-of-phase modulated laser-beam excitation at two discrete wavelengths near the peak λ_A and the baseline λ_B of the target analyte absorption band [16]. WM-DPTR generates two-channel signals, differential amplitude A_{AB} and phase P_{AB} at the fundamental frequency of the Fourier series expansion of the time domain differential signal expressed as.

$$S_{AB} = \begin{cases} S_A(t); & 0 \le t \le \tau_p \\ S_B(t) - S_A\left(t - \frac{\tau_0}{2}\right) + S_B\left(t - \frac{\tau_0}{2}\right); & \frac{\tau_0}{2} \le t \le \tau_0 \end{cases} \quad (1)$$

where $S_A(t)$ and $S_B(t)$ are single-wavelength photothermal radiometry (PTR) signals at wavelength λ_A and λ_B, respectively, τ_0 is the modulation period, and τ_p is the laser pulse duration [15]. Because the baseline variation is eliminated through real-time differential measurements, the signal dynamic range and signal-to-noise ratio (SNR) are greatly increased. One unique aspect of WM-DPTR is that the signal sensitivity and dynamic range can be optimally tuned through two system baseline parameters (without analyte): amplitude ratio $R = A_A/A_B$ and phase shift $\Delta P = P_A - P_B$. WM-DPTR can be applied to glucose detection when the two beam wavelengths are set at the peak (λ_A = 9.67 µm) and baseline (optimal λ_B ~ 8.5 µm) of the main MIR glucose absorption band, Fig. 1.

2.2 Experimental setup

As presented in Fig.2, two 180°-out-of-phase square-wave modulated laser beams at the peak and baseline wavelengths of glucose irradiate the sample (finger). The collimated laser beam size is 2 x 2.4 mm. The generated infrared emission from the sample is collected and focused onto the detector by a pair of parabolic mirrors. The thermophotonic signal is sent to a lock-in amplifier for demodulation. A computer controls laser modulation, data acquisition and processing. Laser output power at pulse duty cycle (DC) 5% is ~ 3.4 mW with single wavelength measurements and ~ 6.8 mW with differential wavelength measurements. A Quasi-CW wavelength modulation methodology involving a low-frequency square-wave modulation envelope was developed and presented elsewhere [21], where a tunable QCL switches between peak wavelength (9.6 µm) and baseline wavelength (8.25 µm) at a frequency half the modulation frequency.

2.3 In vivo measurement protocols

The *in-vivo* measurements were designed to generate data from various blood glucose concentrations (BGC) in volunteers and test the corresponding variations in the WM-DPTR signals. First, two nondiabetic volunteers (Sub. 1 and Sub. 2) and one diabetic volunteer (Sub. 3) fasted before the measurements long enough to attain a low glucose level. In order to increase the BGC difference among the subjects, one of the nondiabetic volunteers (Sub. 2) exercised before the measurements and the diabetic subject did not consume insulin so as not to hide the subject's natural disability to metabolize glucose. Then, OGTT was introduced and Sub. 1 showed an increase in glucose level followed by normal decrease, thus yielding normal sensitivity and normal glucose range data. The exercised Sub. 2 showed a higher glucose level due to insulin blockers being switched on during the immediately prior exercise. Thus, the glucose meter gave a larger top concentration and a wider BGC range. Finally Sub.3, being diabetic, showed a very high concentration over the working range of the commercial meter and expected low rates of glucose consumption.

WM-DPTR OGTT included *in vivo* WM-DPTR measurements and simultaneous BGC measurements as reference before and after glucose dose intakes. OGTT is a method to help diagnose instances of diabetes mellitus or insulin resistance, in which a glucose dose is administered and blood samples are taken afterward to determine how quickly the glucose is cleared from the

blood [22]. Glucose dose was determined using the WHO standard: 75 g glucose powder in 250 ml water, consumed in a 5-min window. The aim of WM-DPTR OGTT measurements was to see how WM-DPTR signals respond to the controlled blood glucose concentration variations during OGTT. Initial Ethics approval and Laser Safety approval from the Research Office and the Laser Safety Office of the University of Toronto was received for the study and consent was obtained from each volunteer.

Three volunteers with different diabetic histories and fasting conditions participated in the tests to cover a wide BGC range. Sub. 1, nondiabetic, fasted for 19 hours, aimed for normal BGC range; Sub. 2, nondiabetic, fasted for 18 hours, and exercised for 1.5 hours, aimed for increased BGC dynamic range [23,24]; Sub. 3, Type-I diabetic, fasted for 14 hours without insulin injection, aimed for high BGC level range. Type 1 diabetes is characterized by deficient insulin production and requires daily administration of insulin.

In the WM-DPTR measurements, wavelength pairs λ_A = 9.60 μm and λ_B = 8.25 μm were used instead of λ_A = 9.67 μm and λ_B = 8.5 μm, as they corresponded to better laser output power efficiency. In order to reach the ISF in the basal layers [25], the laser was modulated at 5 Hz with ~ 36 – 67 μm probing depth in the epidermis. The probing depth range was estimated based on the two boundary skin thermal diffusivity values at water content 10% and 60% in the epidermis layer [20]. In contrast, the optical penetration depth in skin at the glucose sensitive wavelength (~ 9.6 μm) is only ~ 20 μm. Laser power on the dorsal part of the middle finger under the nail of the subject's right hand was ~ 6.74 mW, below the skin-safe standard Maximum Permissible Exposure (MPE) (7.45 mW for the laser beam size) [26]. The site was chosen because of its flat curvature and thin stratum corneum (SC) (< 18 μm) [27], and the small SC thickness variation between different people, see Section 3 for details. Single wavelength (λ_A = 9.60 μm) measurements (amplitude A_A and phase P_A) were also made for a comparison with the differential measurements. Simultaneous finger temperature readings were obtained near the measurement site with a thermocouple attached to the subject's finger. Finger pricking BGC measurements were performed on 10 different finger tips, each at the beginning of the WM-DPTR measurement set with a glucometer (OneTouch Verio Flex). The entire WM-DPTR OGTT (BGC + WM-DPTR) measurements lasted for ~ 3.5 hours with 20-minute intervals, starting with the fasting measurement set.

For the measurements in this paper, R and ΔP were fixed throughout the measurements involving each subject, with small differences between subjects.

Two sets of additional measurements were performed for verification of WM-DPTR principle: (1) negative control measurements were performed on Sub. 1 under similar fasting conditions in which the 250 ml glucose dose was replaced with the same amount of pure water; (2) differential measurements with a glucose-insensitive pair of wavelengths (9.56 μm and 9.77 μm) were performed on Sub. 2 during OGTT. The two wavelengths were selected such that glucose has large but equal absorption coefficients.

3. Results and discussion

Figure 3 displays the *in vivo* WM-DPTR and the BGC measurement results of Sub.1. In Fig. 3(a), the time profile of the differential phase P_{AB} (normalized) is plotted together with the simultaneously measured blood glucose concentration BGC ranging from 5.3 mmol/L to 12.2 mmol/L, with the glucometer error being 0.83 mmol/L when BGC < 5.55 mmol/L; and 15% when BGC > 5.55 mmol/L. The BGC increases immediately after the glucose dose intake, peaks at 80 min and then falls back below 7 mmol/L after 160 min. The first datum was measured before the onset of glucose dose intakes. It can be seen that the phase curve is well correlated with BGC (0.95 correlation coefficient), following the rising and falling trend of BGC with large dynamic range (~ 77° in phase change). Due to the fact that the blood glucose concentration was in a very dynamic state during OGTT, measurement error bars were not statistically meaningful and were not plotted here. However, the signal error could be estimated from the stationary fasting measurements during which the blood glucose level was relatively stable. It should be noted that unlike the single-ended PTR method, WM-DPTR signal errors are R and ΔP dependent. The most sensitive setting R = 1 and ΔP = 180° will result in the largest error because the differential amplitude is zero and differential phase is prone to 180° transition (Mandelis and Guo, 2014). In order to obtain reasonable SNR, the glucose sensitivity must be somewhat compromised. With this consideration, R was set close to 1 and ΔP close to 180° where the differential amplitude error was ~ 6.6%, and the differential phase error was ~ 2.6°. Compared with the BGC curve, the differential phase exhibits a delay in the rising part of the curve. This is most likely due to the lag between ISF glucose concentration and BGC. Comparison between the differential phase P_{AB} and the blood glucose concentration BGC in OGTT measurements and the negative control measurements of Sub. 1 are shown in Fig. 3(b) (differential phase P_{AB}) and in Fig. 3(c) (blood glucose concentration BGC). It can be seen that P_{AB} and BGC have significant difference in OGTT and the control measurements, with P_{AB} peaking at 80 deg (OGTT) compared to 20 deg (control) and 12 mmol/L (OGTT) compared to5.7 mmol/L (control) for

BGC. The differential phase P_{AB} rise after 80 min in the control measurements could be correlated with the single-point rise of BGC at 120 min, which implies higher WM-DPTR glucose sensitivity than the glucometer (0.8 mmol/L error in this range). The control measurements have established that the measured changes in the differential phase correlated with glucose in OGTT were not due to a fluid volume change.

In contrast, the single wavelength amplitude A_A and phase P_A of Sub.1, shown in Figs. 4(a) and 4(b), do not correlate with BGC, but the amplitude is strongly correlated with the finger temperature (0.86 correlation coefficient), Fig. 4(c), a parameter influenced by many other factors besides BGC. This test amply demonstrates the advantage of differential WM-DPTR in ISF glucose detection over the conventional single wavelength PTR method.

The system parameters R and ΔP were optimally tuned for the phase channel in Fig. 3. They could also be tuned optimally for both amplitude and phase channels, but with some trade-off in sensitivities as shown in the measurements of Sub. 2, Fig. 5. It can be seen that both differential phase P_{AB}, Fig. 5(a), and differential amplitude $A_{AB,}$ Fig. 5(b), are correlated (with risetime delays) with the BGC. However, it is noted that the phase dynamic range is smaller (~39°) than that in Fig. 3 (~77°), even with the larger BGC range (4.6 mmol/L to 17.7 mmol/L). Figure 5(c) displays the BGC response of the simultaneously measured differential phase P_{AB}, but with a glucose-insensitive wavelength pair (9.56 μm and 9.77 μm). It is clearly shown that P_{AB} is not correlated to BGC, thereby validating the high differential absorption specificity of WM-DPTR in addition to R- and ΔP-dependent sensitivity.

Glucose sensitivity of WM-DPTR spans a large BGC range. Figure 6 shows the measurement results of Sub. 3. As a type I diabetic who can only produce little or no insulin to clear the blood stream from glucose, Sub. 3's BGC became too high to be measured (outside the 33.2 mmol/L glucometer range) between 60-140 min. On the contrary, the differential phase follows the measured BGC pattern with a delay where data are available and reasonably tracks the full response range, including the (missing BGC) peak. In order to measure BGC accurately over a wide range beyond the glucometer range, a YSI glucose analyzer can be used for BGC measurements, but the WM-DPTR method shows that its dynamic range is adequate for tracking the glucose ISF concentration of diabetic patients.

In order to evaluate any variation in WM-DPTR measurements due to different measuring site and different skin color in realistic glucose detection, two sets of *in vivo* background measurements were performed to check the stability of the two system parameters amplitude ratio R and phase shift ΔP, which determine the repeatability of WM-DPTR signals. The aim of the first set of measurements was to check for measurement location signal dependence. The measurements were performed at four locations on the right hand of a subject (BGC ~ 5.1 mmol/L over the measurement period): L1, back of the middle finger under the nail; L2, index finger tip; L3, thumb; L4, palm edge. Each location was measured five times and the R and ΔP average AV and standard deviation SD were calculated and listed in Table 1. It is seen that the amplitude ratio R and phase shift ΔP varied from location to location, 1.08 to 1.14 for R and 177.39 deg to 182.57 deg for ΔP. The location dependence might be due to the variation in SC thickness. The thicker SC in L2 and L3 generated larger R and ΔP. SC thickness at L2, L3 and L4 can be very different from person to person, depending on the use of their hands, for instance, the hand of a manual worker (a mechanic) and that of a lawyer. On the contrary L1 is usually free of wear and tear for most people and their SC thickness is similar. Considering the small person-to-person variance and small SC thickness, L1 is the optimal location for measurements. The aim of the second set of background measurements was to check for skin color dependence. L1 location of three subjects (BGC ~ 6 mmol/L) with different skin colors (white, yellow and dark) were measured five times each and the results are listed in Table 2. The inter-color (three colors) and intra-color (five measurements for each color) values of amplitude ratio and phase shift are the same within variance, thereby concluding that WM-DPTR signals are skin color independent.

The clinical significance of a glucose sensing method is usually assessed using Clarke Error Analysis [28], the analysis of the uncertainty of predicted BGC. However, this is not the goal of the present paper which focuses on detection feasibility. In order to produce a clinically acceptable data analysis, WM-DPTR signals must be properly calibrated with BGC reference measurements with more volunteers than the present study. This will be the goal of the next phase of the WM-DPTR glucose biosensor evaluation. Nevertheless, the glucose sensitivity of the WM-DPTR method can be demonstrated through the phase signal channel vs. blood glucose concentration plots illustrated in Fig.7: Fig. 7(a) for Sub.1 and Fig. 7(b) for Sub 2. Here, the differential phase (y-axis) reflects the measured WM-DPTR phase dependence on interstitial fluid glucose concentration, while the x-axis is the measured finger-pricking blood glucose concentration during the glucose intake period of the OGTT process. For ease of comparison, the phase is normalized to zero at BGC = 5.3 mmol/L. Figure 7 exhibits the increase of $P_{AB,}$ with BGC for both subjects. In addition, the phase readings of Sub.1 rise faster with, and are more sensitive to, glucose intake than those of Sub. 2 in the BGC range 5.3 – 12.3 mmol/L. This

person-to-person variation is the result of the fact that the R and ΔP settings (figure insets) for Sub. 1 are better than those for Sub.2. R is closer to 1 for Sub.1 resulting in higher sensitivity. Following the end of glucose intakes, the data for the P_{AB}-BGC relationship during the glucose metabolism and signal transient toward the return to the baseline were shifted to the left (not shown here) of the intake curves of Fig. 7. This is as expected from the well-known time lag of glucose diffusion into the ISF [29,30]. It is the challenge each body-fluid-mediated glucose detection technique encounters during fast-glucose-change time intervals such as OGTT. Special calibration is needed as for the MINIMED 670G SYSTEM, the currently used minimally-invasive glucose sensor by Medtronic. These fast transient phenomena present an interesting and possibly important venue for WM-DPTR to study the glucose diffusion process in and out of the interstitial fluid following penetration into the blood stream. They also point to a more complicated calibration curve generation procedure for the WM-DPTR glucose biosensor.

4. Conclusions

In vivo noninvasive WM-DPTR measurements were performed on the finger of three diabetic and nondiabetic volunteers in the MIR range that included the glucose fundamental absorption band. The WM-DPTR measurements were carried out under controlled glucose concentrations during oral glucose tolerance testing, with finger pricking BGC measurements as reference. The strong correlation between the WM-DPTR signal and the BGC measurements demonstrated that WM-DPTR can be used to perform accurate and precise noninvasive glucose detection in the ISF. The differential phase of WM-DPTR exhibited large dynamic range (77°) and higher glucose concentration sensing limit than a commercial glucometer (33.2 mmol/L). Our initial *in vivo* measurements with optimal measurement site, verified by negative control measurements and color-blind tests, have revealed the feasibility of WM-DPTR in noninvasive glucose sensing. In order to evaluate the technology, future work will involve patient trials and more volunteers to generate glucose calibration curves with statistical significance.

Acknowledgements The authors are grateful to the Natural Sciences and Engineering Research Council of Canada (NSERC) for a Discovery Grant to A.M. and to the Canada Research Chairs Program.

References

[1] Global report on diabetes. World Health Organization (2016). http://apps.who.int/iris/bitstream/handle/10665/204871/9789241565257_eng.pdf;jsessionid=2CFA59AEEEB384B9766403EA2A5EA6A2?sequence=1
[2] International Diabetes Federation (IDF) diabetes atlas (2015).
[3] W. M. Ong, S. S. Chua, and C. J. Ng, Patient Prefer Adher. **8**, 237 (2014).
[4] https://www.the-scientist.com/news-analysis/will-the-noninvasive-glucose-monitoring-revolution-ever-arrive-30754.
[5] T. Lin, A. Gal, Y. Mayzel, K. Horman, and K. Bahartan, Curr. Trends Biomed. Eng. Biosci. **6**, 555696 (2017).
[6] S. K. Vashist, Anal. Chim. Acta. **750**, 16 (2012).
[7] N. S. Oliver, T. Toumazou, A. E. G. Cass, and D. G. Johnston, Diabet. Med. **26**, R49 (2009).
[8] A. Bauer, O. Hertzberg, A. Küderle, D. Strobel, M. A. Pleitez, and W. Mäntele, J. Biophotonics **11**, e201600261 (2018).
[9] S. Liakat, K. A. Bors, L. Xu, C. M. Woods, J. Doyle and C. F. Gmachl, Biomed Opt. Express **5**, 2397 (2014).
[10] J. Kottmann, J. M. Rey, and M. W. Sigrist, Seonsor. **16**, 1663 (2016).
[11] C. E. F. do Amaral and B. Wolf, Med. Eng. Phys. **30**, 541 (2008).
[12] J. Kim, A. S. Campbell, and J. Wang, Talanta **177**, 163 (2018).
[13] L. Lipani, B. G. R. Dupont, F. Doungmene, F. Marken, R. M. Tyrrell, R. H. Guy and A. Ilie, Nature Nanotechnology, **13**, 504 (2018).
[14] O. K. Cho, Y. O. Kim, H. Mitsumarki, and K. Kuwa, Clin. Chem. **50**(10), 1894 (2004).
[15] Y. Zhang, J. Zhu, Y. Liang, H. Chen, S. Ying, and Z. Chen, Physiol. Meas. **38**, 325 (2017).
[16] A. Mandelis and X. Guo, US Patent No. 08649835 Cl. 600–316, issued on Feb. 11, 2014.
[17] A. Mandelis and X. Guo, Phys. Rev. E **84**, 041917 (2011).
[18] X. Guo, A. Mandelis and B. Zinman, Int. J. Thermophys. **33**, 1814 (2012).
[19] X. Guo, A. Mandelis and B. Zinman, J. Biophotonics, **6**, 911 (2013).
[20] X. Guo, A. Mandelis and B. Zinman, Biomed. Opt. Exp. **3**, 3012 (2012).
[21] X. Guo, K. Shojaei-Asanjan, D. Zhang, K. Sivagurunathan, Q. Sun, P. Song, A. Mandelis, B. Chen, M. Goledzinowski, Q. Zhou, and F. Comeau, Biomed. Opt. Express, **9**, 4638 (2018).
[22] https://en.wikipedia.org/wiki/Glucose_tolerance_test.
[23] S. H. Knudsen, K Karstoft, B. K. Pedersen, G. van Hall, and T. P. J. Solomon, Physiol Rep. **2** e12114 (2014).
[24] C. A. Titchenal, K. Hatfield, M. Dunn, and J. Davis, Int. J. Sport Nutr. **5** (Suppl 1):, P14 (2008).
[25] W. Groenendaal, G. von Basum, K. A. Schmidt, P. A. J. Hilbers, and N. A. W. van Riel, J. Diabetes Sci. Technol. **4**, 1032 (2010).
[26] American National Standards Institute (ANSI) Z136.
[27] J. Sandby-Møller, T. Poulsen, and H. C. Wulf, Acta Derm Venereol, **83**, 410 (2003).
[28] WL. Clarke, Diabetes Technol Ther. **7**, 776 (2005).

[29] A. Basu, S. Dube, M. Slama, I. Errazuriz, J. C. Amezcua,Y. C. Kudva, T. Peyser, R. E. Carter, C. Cobelli, and R. Basu, Diabetes, **62**, 4083 (2013).
[30] B. J. van Enter and E. von Hauff, Chem. Commun., **54**, 5032 (2018).

Figures

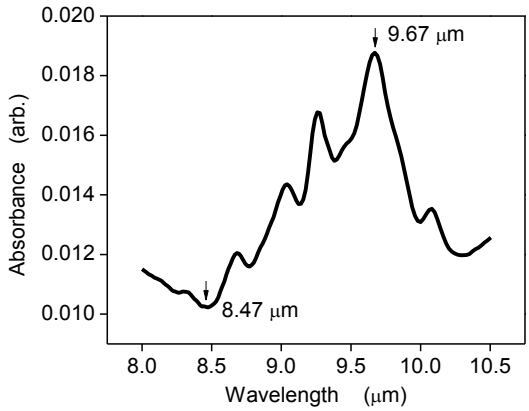

Figure 1 FTIR glucose absorption band in MIR range with main peak at λ_A = 9.67 μm and baseline at λ_B ~ 8.5 μm.

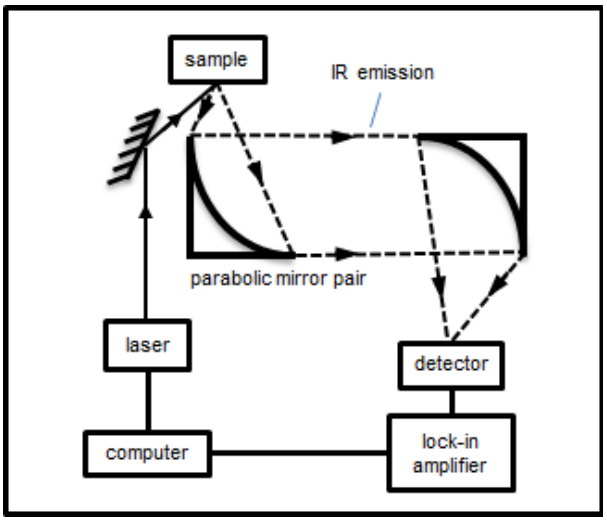

Figure 2 Schematic diagram of WM-DPTR system setup: The modulated laser beam is steered onto the sample surface; the generated IR emission is collected by a MCZT detector through a pair of parabolic mirrors and then sent to the lock-in amplifier for demodulation; the amplitude and phase of the PTR signal are sent to a computer for further processing

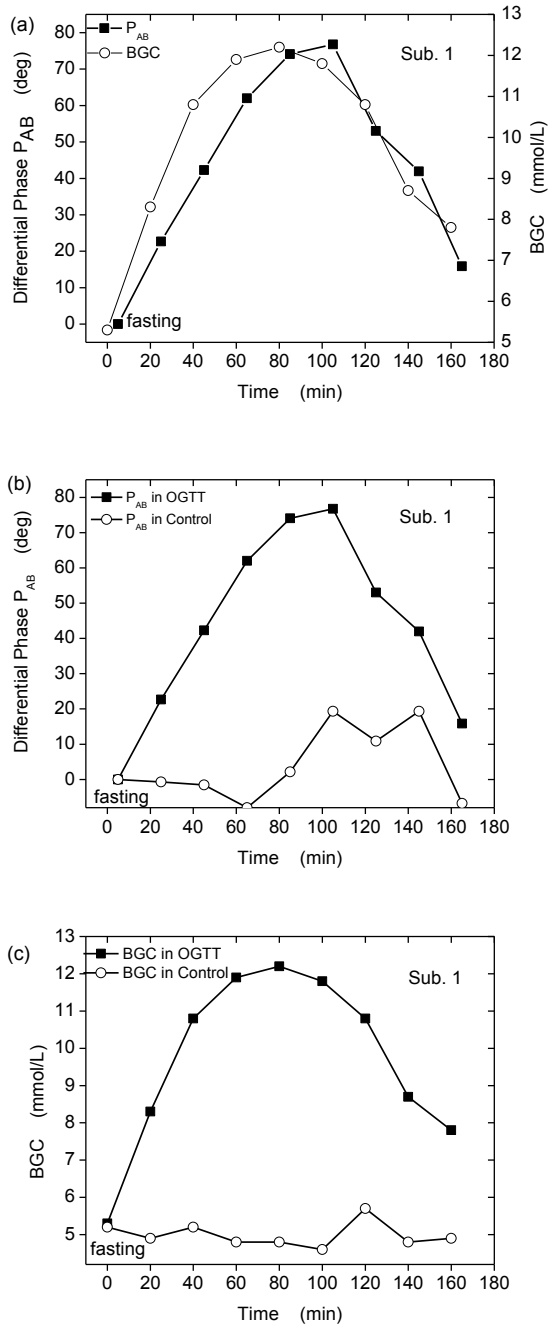

Figure 3 Nondiabetic subject (Sub.1) OGTT time profile of differential phase P_{AB} (solid squares + line) against the BGC reference (open circles + line) (a); time profile comparison of OGTT (solid squares + line) and its control (open circles + line) in differential phase P_{AB} (b); and in BGC (c).

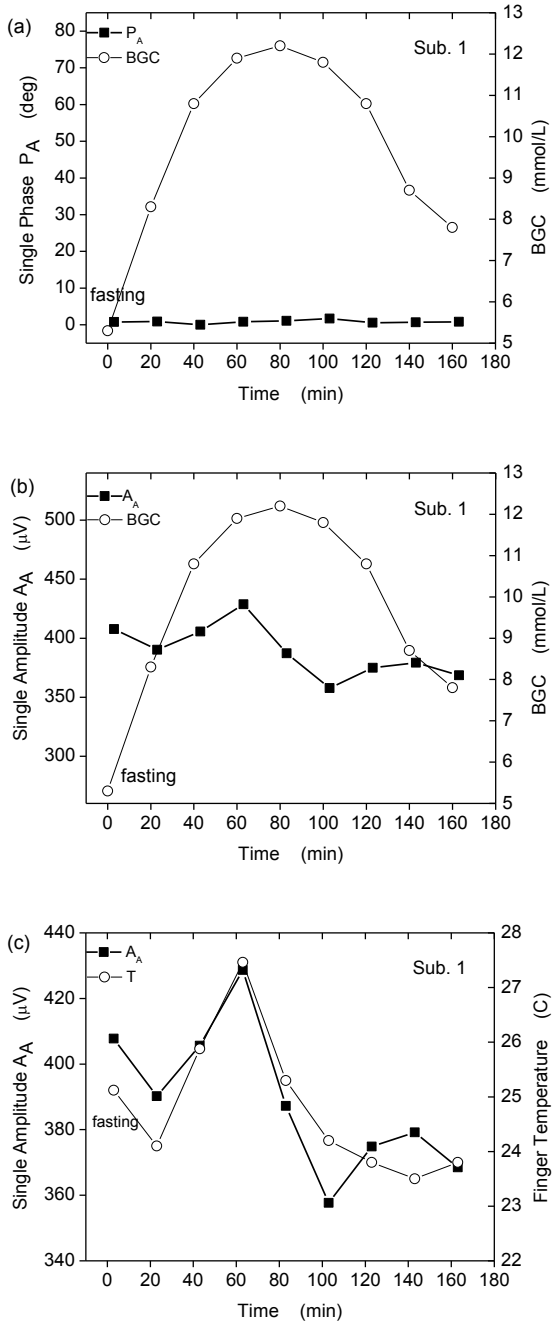

Figure 4 Nondiabetic subject (Sub. 1) OGTT time profile of single-ended signals at peak wavelength λ_A against the reference/finger temperature (open circles + line). (a) single phase P_A against the BGC reference; (b) single amplitude A_A against the BGC reference; (c) single amplitude A_A against finger temperature

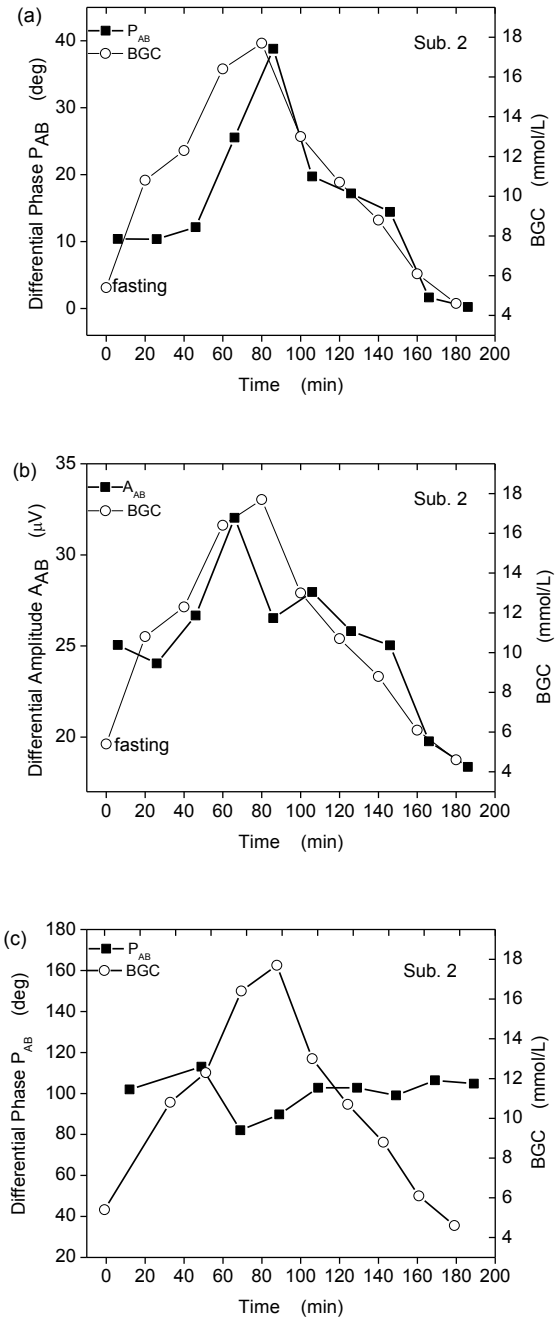

Figure 5 Post-exercise nondiabetic subject (Sub. 2) OGTT time profile of differential signals (solid squares + line) against BGC reference (open circles + line). (a) differential phase P_{AB}; (b) differential amplitude A_{AB}; (c) differential phase P_{AB} measured with the glucose-insensitive wavelength pair 9.56 μm and 9.77 μm.

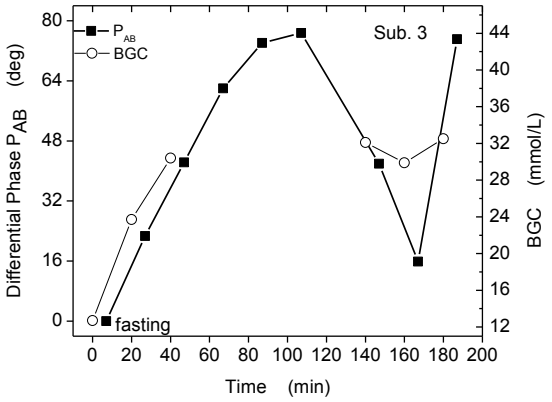

Figure 6 Type I diabetic subject (Sub.3) OGTT time profile of differential phase P_{AB} (solid squares + line) against BGC reference (open circles + line). The missing three BGC reference points between 60 – 120 min was due to overload of the glucometer.

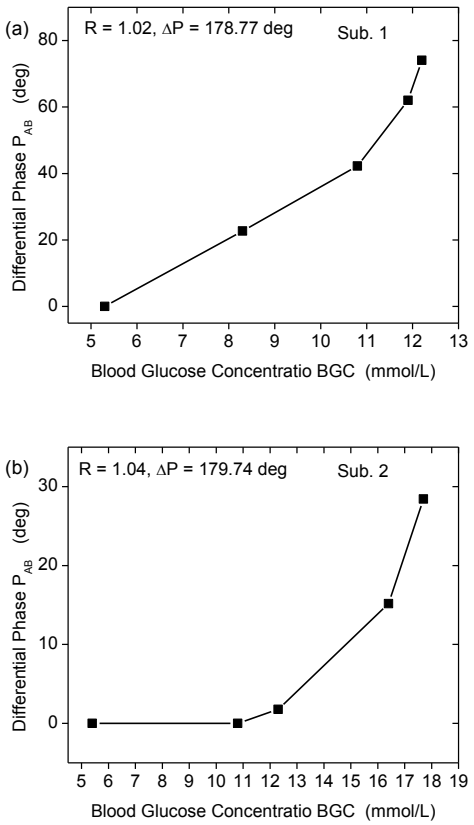

Figure 7 WM-DPTR differential phase P_{AB} versus blood glucose concentration BGC during glucose OGTT intake risetime. (a) Sub.1; (b) Sub. 2.

Tables

Table 1 Location dependence of system parameters R and ΔP

Skin Location	R		ΔP (deg)	
	AV	SD	AV	SD
L1	1.08	0.01	177.39	0.84
L2	1.14	0.00	182.57	0.33
L3	1.14	0.01	182.24	0.27
L4	1.11	0.01	179.91	0.64
Inter-location	**1.12**	**0.03**	**180.53**	**2.40**

Table 2 Color dependence of system parameters R and ΔP

Skin Color	R		ΔP (deg)	
	AV	SD	AV	SD
white	1.08	0.01	177.39	0.84
yellow	1.09	0.02	178.93	0.95
dark	1.10	0.01	179.23	0.28
Inter-color	**1.09**	**0.01**	**178.52**	**0.99**